PROTEINS: Structure, Function, and Bioinformatics 60:803–806 (2005)

STRUCTURE NOTE

Crystal Structure of Stilbene Synthase From *Arachis hypogaea*

Yasuhito Shomura,[1†] Ichiro Torayama,[1‡] Dae-Yeon Suh,[2] Ting Xiang,[3§] Akiko Kita,[1,4] Ushio Sankawa,[3] and Kunio Miki[1,5*]

[1]*Department of Chemistry, Graduate School of Science, Kyoto University, Kyoto, Japan*
[2]*Department of Chemistry and Biochemistry, University of Regina, Regina, Saskatchewan, Canada*
[3]*Toyama Prefecture International Health Complex, Toyama, Japan*
[4]*Research Reactor Institute, Kyoto University, Osaka, Japan*
[5]*RIKEN Harima Institute/SPring-8, Hyogo, Japan*

Introduction. Stilbene synthase [STS; Enzyme Commission (EC) 2.3.1.95] and chalcone synthase (CHS; EC 2.3.1.74) are members of the type III polyketide synthases (PKSs) and plant-specific enzymes.[1] CHS is widely found in higher plants and plays a key role in the flavonoid biosynthesis by supplying chalcone to downstream enzymes. In contrast, a limited number of plants have STS essential for the synthesis of resveratrol utilized in the stilbenoid biosynthesis.[2] The members of CHS superfamily, including STS, produce linear polyketide intermediates by a common catalytic mechanism where coenzyme A (CoA)-linked starter molecules are iteratively condensed by acetyl units from malonyl-CoA.[3] STS and CHS share around 70% sequence identity without significant deletions and insertions; therefore, the enzymatic mechanism of STS has been considered to be very close to that of CHS. STS and CHS catalyze condensation reactions of *p*-coumaroyl-CoA and 3 acetyl units from malonyl-CoA, and produce a common linear tetraketide intermediate. In the following cyclization reaction, however, STS and CHS catalyze aldol and Claisen condensation of the tetraketide, resulting in 2 different final products, resveratrol and chalcone, respectively. The crystal structure and molecular mechanism of CHS from *Medicago sativa* (alfalfa) have recently been reported,[4] but the primary determinant of the cyclization reactions catalyzed by STS and CHS was not clear. More recently, the crystal structure of STS from *Pinus silvestris* (pine) was reported and provided a framework for understanding the specificity in the cyclization reaction.[5] This report describes the crystal structures of STS from *Arachis hypogaea* (peanut) in the absence and presence of its final product resveratrol at 2.4 Å and 2.9 Å, respectively. Detailed structural comparisons of STS from *A. hypogaea* (peanut STS) with STS from *P. silvestris* (pine STS) and CHS (alfalfa CHS) evidently revealed common differences between STS and CHS in the local conformation around the active site pocket.

Materials and Methods. STS from *A. hypogaea* was expressed in *Escherichia coli* BL21 (DE3) pLysS as a Trx (thioredoxin)–Histag (6 × histidine) fusion protein.[6] Following Ni^{2+} affinity purification, the Trx-Histag region was cleaved by enterokinase (Invitrogen; Carlsbad, CA). Further purification was performed with a phenyl Sepharose hydrophobic interaction column and Superdex 200 gel filtration column (Amersham Biosciences, Buckinghamshire, UK). The protein solution was concentrated to 30 mg/mL using a Centriprep YM-10 concentrator (Millipore; Billerica, MA). The apo form of STS (STS-apo) was crystallized at 293 K by the sitting drop vapor diffusion method mixing 3 μL of protein solution [30 mg/mL protein, 50 m*M* potassium phosphate, pH 7.2, 50 m*M* potassium chloride, and 1 m*M* dithiothreitol (DTT)] with 3 μL of the precipitant solution [100 m*M* sodium citrate pH 4.6, 150 m*M* ammonium sulfate, 16% (w/v) polyethylene glycol 6000, and 10% (v/v) glycerol]. Crystals of STS in the complex with resveratrol (STS-resveratrol) were obtained by using a protein solution containing 5 m*M* resveratrol and the same precipitant solution as used for STS-apo crystals. For cryoprotection, the crystals were stepwise transferred into a precipitant solution including 25% (v/v) glycerol and subsequently flash-cooled in a cold nitrogen-gas stream. Diffraction data were collected at SPring-8 beamline BL44B2 and processed using HKL suite.[7] Both the apo- and resveratrol-bound STS crystals belong to space group

Grant sponsor: RIKEN (Junior Research Associate Fellowship to Y. Shomura).

†Current address: Department of Cellular Biochemistry, Max-Planck-Institute of Biochemistry, Martinsried 82152, Germany

‡Current address: Structural Biology Center, National Institute of Genetics, Mishima 411-8540, Japan

§Current address: Laboratory of Natural Product Chemistry, Graduate School of Pharmaceutical Sciences, University of Tokyo, 7-3-1 Hongo, Bunkyo-ku, Tokyo 113-0033, Japan

*Correspondence to: Kunio Miki, Department of Chemistry, Graduate School of Science, Kyoto University, Sakyo-ku, Kyoto 606-8502, Japan. E-mail: miki@kuchem.kyoto-u.ac.jp

Received 27 January 2005; Accepted 28 February 2005

Published online 18 July 2005 in Wiley InterScience (www.interscience.wiley.com). DOI: 10.1002/prot.20584

TABLE I. Statistics of Diffraction Data and Structural Refinement

Data set	STS-apo	STS-resveratrol
Diffraction data		
Space group	$P3_121$	$P3_121$
Cell parameters (Å) *a,c*	100.8, 74.0	100.7, 74.1
Resolution (Å)	57–2.4	57–2.9
Measured intensities	324,636	160,433
Unique reflections	17,189	9,941
Completeness (%)[a]	99.3 (95.1)	92.9 (84.7)
Multiplicity[a]	8.2 (4.8)	7.2 (4.7)
Mean I/σ (I)[a,b]	14.7 (2.1)	9.6 (3.4)
R_{sym} (%)[a,c]	7.1 (24.6)	11.5 (18.7)
Refinement		
Resolution range (Å)	40–2.4	40–2.9
R_{work} (%)[d]	20.6	19.2
R_{free} (%)[d,e]	24.3	25.2
Protein atoms	2982	2988
Solvent atoms	180	87
Ligand atoms	26	30
Deviations from ideality		
RMSD for bond lengths (Å)	0.007	0.007
rmsd for Bond angles (degrees)	1.3	1.3
B-factors RMSD for bonded main-chain atoms (Å^2)	2.0	1.1
B-factors RMSD for bonded side-chain atoms (Å^2)	3.0	1.7
Most favored ϕ–ψ angles (% residues)	90.5	88.4
Disallowed ϕ–ψ angles (% residues)	0	0

[a]Values in parentheses are for highest resolution shells.
[b]Signal-to-noise ratio of intensities.
[c]$R_{sym} = \Sigma(|I - \langle I \rangle|)/\Sigma I$.
[d]$R = \Sigma(|F_o - F_c|)/\Sigma F_o$.
[e]Five percent of reflections were randomly chosen for calculation of free R value.

$P3_121$ and contain a monomer per asymmetric unit (see Table I). The structures were determined by molecular replacement with MolRep[8] using the polyalanine model of alfalfa CHS as a search model. Further model correction and structure refinement were iteratively carried out using O[9] and Crystallography & NMR system (CNS).[10] The final model of STS-apo contains 2982 protein atoms (residues 2–389), 2 citric acid molecules, and 180 solvent atoms. The same region of the polypeptides, a resveratrol molecule and 87 solvent atoms, were included in the model of STS-resveratrol. The final R of STS-apo and STS-resveratrol are 20.6% (R_{free} 24.3%) and 19.2% (R_{free} 25.2%), respectively. Root-mean-square deviations (RMSDs) for C_α positions were calculated with LSQMAN[11] for each subunit in asymmetric units. The coordinates and structure factors have been submitted to the Protein Data Bank (PDB accession codes, 1Z1E and 1Z1F).

Results and Discussion. STS is a homodimeric protein composed of 43 kDa subunits that are related by a crystallographic dyad in the crystal structures [Fig. 1(A)]. Bound resveratrol molecules in the STS-resveratrol structure are clearly observed for the first time [Fig. 1(B)]. No remarkable conformational changes occurred around the active site pocket upon the binding of resveratrol, with the exception that the side-chain of Phe265, which is disordered in the STS-apo structure, is clearly visible in the STS-resveratrol structure [Fig. 1(B)], as seen in other structures of related enzymes.[1] The overall structure of peanut STS is highly homologous to that of alfalfa CHS, as revealed by the RMSDs of 0.53 Å and 0.62 Å (calculated for 2 subunits in the asymmetric unit of the alfalfa CHS structure) for the 386 C_α positions. Unexpectedly, RMSDs from 0.62 Å to 0.70 Å (calculated for 6 subunits in the asymmetric unit of the pine STS structure) between the structures of peanut STS and pine STS for the 386 C_α positions were comparable with the values between the structures of peanut STS and alfalfa CHS, indicating a relatively high diversity in the tertiary structures of STS from different species. The plot of RMSD as a function of sequential residue number (data not shown) indicates that 3 areas, 133–136 (a1), 248–256 (a2), and 265–269 (a3), are particularly divergent between the structures of peanut STS and alfalfa CHS [Fig. 1(A)]. Considering the effect by crystal packing, however, a2 and a3 are close to a neighboring molecule in the crystals, and it is still not clear whether the divergences observed at a2 and a3 result from the crystal-packing contact or intrinsic conformational differences. Of the 3 areas, a1 and a2 show high RMSDs between the structures of peanut STS and pine STS as well. For the area a1, Austin et al.[5] recently suggested that Thr132 in the area plays a critical role as a functionally relevant residue for the cyclization reaction of the tetraketide intermediate by furnishing STS with a thioesterase-like activity. While Thr132 is a highly conserved residue among the members of CHS superfamily [Fig. 1(C)], the positional difference significantly affects the hydrogen-bond network around the catalytic cysteine, which determines the manner for the cyclization reaction according to their model. The position of Thr132 is highly homologous between 2 STS structures, and in analogy to pine STS, the hydroxyl group in the side-chain of peanut STS seems to contribute to the hydrogen-bond network between Glu192 and Ser338 through a water molecule, which is not observed in the structure of alfalfa CHS [Fig. 1(D)]. Besides, the downstream region (residues 133–135) is considerably divergent, as indicated by the maximum RMSD of 2.5 Å in spite of the high similarity between peanut STS and CHSs in the amino acid sequence [Fig. 1(C)]. Therefore, the difference between STS and CHS in the conformation around a1 is likely to be caused by another region, rather than to exist per se. A more extended comparison between the structures of peanut STS and alfalfa CHS revealed that the side-chain of Met98 directly affects the structural displacement in the area (a1) by its steric hindrance [Fig. 1(D)]. However, it is still not clear if the only substitution of this residue is enough for functional conversion between STS and CHS, or if additional substitutions are required, because the conformation of the main-chain around the residue also seems to be critical, in addition to the bulkiness of the side-chain. We have also found that the single substitution of Gly255 with bulkier residues remote to this region of peanut STS results in a functional conversion of STS to CHS (to be published). Therefore, there seems to be more factors that determine the manner for the cyclization reaction. Further biochemical studies with mutagenesis

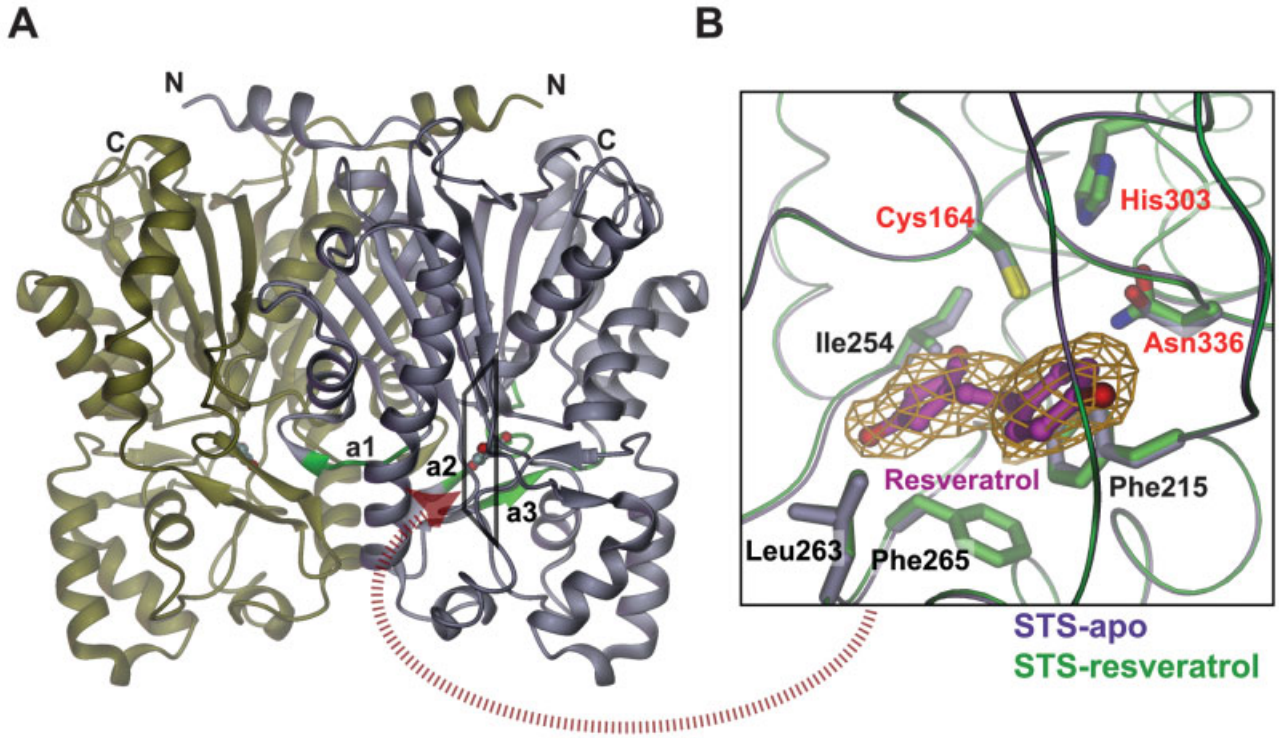

C

	95									105
peanut STS	E	D	M	M	I	R	E	V	P	R	V
pine STS	Q	A	M	L	A	A	E	V	P	R	L
alfalfa CHS	Q	D	M	V	V	V	E	V	P	R	L
pine CHS	Q	D	M	V	V	V	E	V	P	R	L

	130									140
peanut STS	C	T	T	S	G	V	A	L	P	G	V
pine STS	C	T	T	T	T	P	D	L	P	G	A
alfalfa CHS	C	T	T	S	G	V	D	M	P	G	A
pine CHS	C	T	T	S	G	V	D	M	P	G	A

a1

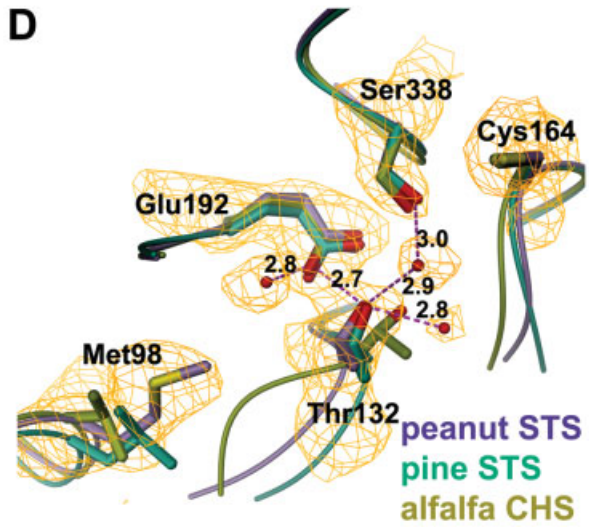

Fig. 1. (**A**) Ribbon diagram of the homodimeric structure of peanut STS-resveratrol with each monomer colored separately. Bound resveratrols are depicted in ball-and-stick models. Structurally divergent areas, a1, a2, and a3, are highlighted in green in the right monomer, and the N- and C-termini are labeled. Figures are produced with DINO[12] and POV-Ray.[13] (**B**) Enlarged view of the active site pockets in STS-apo and STS-resveratrol in the indicated colors. An $F_o - F_c$ difference Fourier electron density map calculated with data from a resveratrol-derivative crystal is indicated in brown (contoured at 1.5 σ), and the refined model of resveratrol is depicted in magenta. Catalytic-triad residues[4] (Cys164, His303, and Asn336) are indicated in red characters. (**C**) Sequence alignments around Met98 and Thr132 for peanut STS1 (GeneBank accession code: AB027606), pine STS1 (Swiss-Prot accession code: P48407), alfalfa CHS2 (Swiss-Prot accession code: P30074), and pine CHS1 (Swiss-Prot accession code: O65872). Unvaried residues are colored in red. The residues belonging to a1 is enclosed with a blue frame. (**D**) Comparison among the structures of peanut STS, pine STS (PDB code: 1U0U, chain A), and alfalfa CHS (1BL5, chain A) around the area a1. Each model is indicated in a different color, and water molecules found in the peanut STS structure are depicted with red balls. An $F_o - F_c$ difference Fourier electron density map calculated with data from a peanut STS-apo crystal, and the model without waters and corresponding residues is indicated in orange (contoured at 1.8 σ). The hydrogen-bond network found in the peanut STS structure is indicated with dotted lines of magenta and the bond lengths are shown in Angstrom units.

and structural studies on related enzymes will elucidate the mechanism of each enzyme in greater detail.

Acknowledgments. Our thanks to Dr. S. Adachi and Mr. T. Matsu for their assistance during data collection at BL44B2, SPring-8.

REFERENCES

1. Austin MB, Noel JP. The chalcone synthase superfamily of type III polyketide synthases. Nat Prod Rep 2003;20:79–110.
2. Tropf S, Lanz T, Rensing SA, Schröder J, Schröder G. Evidence that stilbene synthases have developed from chalcone synthases several times in the course of evolution. J Mol Evol 1994;38:610–618.
3. Kreuzaler F, Hahlbrock K. Enzymic synthesis of an aromatic ring from acetate units: partial purification and some properties of flavanone synthase from cell-suspension cultures of *Petroselinum hortense*. Eur J Biochem 1975;56:205–213.
4. Ferrer JL, Jez JM, Bowman ME, Dixon RA, Noel JP. Structure of chalcone synthase and the molecular basis of plant polyketide biosynthesis. Nat Struct Biol 1999;6:775–784.
5. Austin MB, Bowman ME, Ferrer JL, Schröder J, Noel JP. An aldol switch discovered in stilbene synthases mediates cyclization specificity of type III polyketide synthases. Chem Biol 2004;11:1179–1194.
6. Suh DY, Fukuma K, Kagami J, Yamazaki Y, Shibuya M, Ebizuka Y, Sankawa U. Identification of amino acid residues important in the cyclization reactions of chalcone and stilbene synthases. Biochem J 2000;350:229–235.
7. Otwinowski Z, Minor W. Processing of X-ray diffraction data collected in oscillation mode. Methods Enzymol 1997;276:307–326.
8. Vagin A, Teplyakov A. An approach to multi-copy search in molecular replacement. Acta Crystallogr D Biol Crystallogr 2000; 56:1622–1624.
9. Jones TA, Zou JY, Cowan SW, Kjeldgaard. Improved methods for building protein models in electron density maps and the location of errors in these models. Acta Crystallogr A 1991;47:110–119.
10. Brünger AT, Adams PD, Clore GM, DeLano WL, Gros P, Grosse-Kunstleve RW, Jiang JS, Kuszewski J, Nilges M, Pannu NS, Read RJ, Rice LM, Simonson T, Warren GL. Crystallography & NMR system: a new software suite for macromolecular structure determination. Acta Crystallogr D Biol Crystallogr 1998;54:905–921.
11. Kleywegt GJ, Jones TA. Detecting folding motifs and similarities in protein structures. Methods Enzymol 1997;277:525–545.
12. Philippsen A. DINO: visualizing structural biology. 2003. Available online (http://www.dino3d.org).
13. Team POV-Ray: Persistence of Vision Raytracer. 1997. Available online (http://www.povray.org).